Published in Physical Review B 55, issue 23, 15895-15904, 1997
which should be used for any reference to this work

Local heteroepitaxy of diamond on silicon (100): A study of the interface structure

E. Maillard-Schaller,* O. M. Küttel, P. Gröning, O. Gröning, R. G. Agostino, P. Aebi, and L. Schlapbach
Institut de Physique, Université de Fribourg, Pérolles, CH-1700 Fribourg, Switzerland

P. Wurzinger and P. Pongratz
Institut für Angewandte und Technische Physik, TU Wien, 1040 Vienna, Austria

An extensive study of the interface between highly oriented chemical vapor deposition diamond films and silicon has been performed using atomic force microscopy (AFM), high-resolution scanning electron microscopy (HRSEM), x-ray photoelectron diffraction (XPD), and transmission electron diffraction. The initial roughness of the silicon substrate has been investigated by AFM. Hydrogen plasma has been found to produce pits on the biased substrate surface. The local order of the β-SiC grown on silicon (100) during the bias-enhanced nucleation step has been investigated by XPD through the C 1*s* and the Si 2*p* intensity modulations. Differences in the XPD diffraction features have been studied and found to be due to the element and energy dependence of the scattering effect. The preferential orientation of the diamond nuclei with respect to the silicon substrate has been quantified by comparison of HRSEM pictures and XPD patterns. Only 30–40 % of the crystallites have been found to be oriented relative to the substrate at an early growth stage of a highly oriented diamond film. The partial heteroepitaxy of the diamond nuclei has been confirmed by transmission electron microscopy through electron diffraction and bright- and dark-field images. Simulations of the XPD patterns induced by tilted and azimuthally rotated diamond crystallites have been performed in order to reproduce the smeared-out features of the experimental diffractograms. The short-range order of the diamond lattice at this early growth stage has been found. The amount of carbon on the silicon substrate has been measured by x-ray photoelectron spectroscopy and HRSEM. Comparing the results, we postulated the existence of carbon domains which are too small to be or become diamond nuclei and are etched away by the hydrogen plasma during the growth process.

I. INTRODUCTION

During the past decade significant progress has been made in the growth of oriented diamond films. The microwave plasma enhanced chemical vapor deposition (CVD) has proved to be an efficient deposition technique. By a bias-enhanced nucleation step, good quality diamond is grown on silicon substrates.[1–3] Textured diamond films deposition[3] has been followed by the growth of diamond films which were partially oriented with respect to the substrate.[4] At present, diamond films are grown on silicon (100) with more than 80% of oriented crystallites relative to the silicon substrate.[5–7] However, a 5° to 10° tilt of the diamond crystallites relative to the silicon lattice is always observed.[8,9]

Due to the lack of appropriate investigation techniques very few studies have been done on the orientation of the early growth stage of polycrystalline diamond films. Most studies include scanning electron microscopy (SEM),[5,10] atomic force microscopy[11] (AFM), or transmission electron microscopy (TEM).[12] The limited magnification power of SEM does not allow us to study the very early diamond growth stage but can give quantitative information about the amount of oriented diamond crystallites on the surface after less than one hour of growth. The problem of AFM investigations is the tip convolution effect which does not allow a sharp imaging of crystallites smaller than 0.3 μm in diameter.[13] Despite its high resolution, TEM suffers from the lack of statistics. In addition, the sample preparation is very time consuming.

SEM studies by Stoner *et al.*[5] have shown that only 50% of the diamond grains were oriented relative to the silicon substrate after the bias-enhanced nucleation step.[5] This misorientation is due to the large concentration of misfit dislocations at the diamond/silicon or diamond/SiC interface because of the large mismatch between the two lattices.

In this study, we used AFM to investigate the initial roughness of the silicon substrate. We compared x-ray photoelectron spectroscopy (XPS), x-ray photoelectron diffraction (XPD), and TEM investigations to study the very early stage of oriented diamond growth on silicon. As opposed to TEM, XPS and XPD are nonlocal probes but allow a chemical investigation of the top 40 Å of the sample surface. We will show that investigations by these three techniques show a rather weak percentage of oriented nuclei at an early stage of growth. After 15 h of growth, the diamond film shows a very good orientation as measured by SEM and x-ray diffraction (XRD).

We recently proved that heating the silicon substrate in a CH_4/H_2 plasma to 800 °C is sufficient to grow SiC oriented with respect to the substrate and that the orientation of the SiC layer or SiC islands is independent of the use of a bias during the pretreatment.[14] While this previous paper focused on the influence of the nucleation parameters on the orientation of the SiC layer and the diamond nuclei at the beginning of the deposition process, the present paper deals with an enlarged interface study of CVD diamond on silicon.

First, the roughness of the silicon surface at the beginning of the growth process will be investigated by AFM. Then,

we will show that the local order of the β-SiC grown on silicon (100) can be studied by XPD, investigating either the C 1*s* or the Si 2*p* intensity modulations. Differences between the carbon and the silicon related XPD patterns will be discussed.

The smeared out features of the experimental diffractograms will be explained in terms of the percentage of early oriented diamond nuclei. Simulations of the tilted and azimuthal rotated diamond nanocrystallites will be shown. Comparing XPS and high-resolution scanning electron microscopy (HRSEM) measurements we will finally postulate the existence of nondiamond carbon domains at an early stage of growth.

II. EXPERIMENT

Low-pressure diamond growth was performed on silicon (100) substrates via microwave plasma chemical vapor deposition in a tubular deposition system. Silicon substrates were cleaned in acetone, introduced in the plasma system, and the deposition was started after the pressure in the chamber reached 10^{-6} mbar. Nucleation was induced by applying a dc bias of -225 V to the substrate in a 2% CH_4/H_2 gas mixture plasma and the deposition parameters were chosen in order to get an oriented growth of diamond on silicon (100) (845 °C, 1% CH_4 in H_2). For early growth studies the oriented diamond deposition was stopped after 10 min in order to get individual crystallites with a reasonable size (60–90 nm in diameter). The surface morphology was measured by AFM (Nanoscope III, Digital Instrument Inc.). The samples were scanned with conventional pyramidal Si_3N_4 tips in the taping mode. The roughness of the surface was estimated by root-mean-square (RMS) value calculations. The conductivity of the surface was investigated by a combination of AFM and STM. We used conventional AFM tips which were covered by a thin sputtered gold layer (200 Å). While scanning the surface in the contact mode, a bias was applied to the sample and the current flowing from the conducting tip to the sample was measured and displayed as a current map.

HRSEM was performed in a Hitachi S-900 in-lens field-emission microscope. The primary accelerating voltage was 30 kV for high magnification and the beam current was 2×10^{-11} A. The samples were cooled to 188 K in order to avoid contamination.

X-ray diffraction measurements were performed in a Siemens D5000 diffractometer using the Cu $K\alpha$ radiation and choosing the [111] diamond reflection. The pole figures were obtained by scanning the polar angle from 0° to 80° and the azimuthal angle over half a circle (0°–180°). In order to determine the full width at half maximum of the intensity maxima, the angular step was 1° for both angles.

Transmission electron diffraction (TED) studies were performed in a 200-kV Siemens TEM with a resolution of 0.21 nm. Only plan-view specimens were used here because the preparation of cross-sectional specimens (for high-resolution TEM) has been hindered by a defect rich interface.

The XPD experiments were performed in a VG ESCALAB Mark II spectrometer modified in order to enable motorized sequential angle-scanning data acquisition[15] and equipped with a Mg $K\alpha$ (1253.6 eV) and Si $K\alpha$ (1740.0 eV) twin anode. In order to scan the electron emission direction relative to the crystal axes, the samples were fixed on a goniometric manipulator which is capable of polar ($0°<\theta<90°$) and azimuthal ($0°<\phi<360°$) motions. By rotation of the crystal, 3500 individual XPS spectra have been recorded and fitted.[16] The data are stereographically projected on a plane and represented in a gray scale, with maximum and minimum intensities as white and black, respectively.

Several theoretical approaches have been developed for describing photoelectron diffraction.[17] We apply the single scattering cluster (SSC) theory which was first derived by Lee[18] and then implemented by Kono *et al.*[19] The intensity from one particular photoemitter is calculated as the square of a coherent sum of a primary, unscattered photoelectron wave amplitude, and singly scattered amplitudes from all neighboring atoms in a cluster representing the crystalline order of the sample. The form used here takes into account the exact spherical wave form of the photoelectron wave at the scatterer site by using site-dependent effective complex scattering factors. The power of the SSC calculations in describing the experimental diffraction in natural diamond has been proved by Küttel *et al.*[20]

III. RESULTS

P-doped silicon (100) samples were first heated to 780 °C in a hydrogen plasma during 3 min. Diamond nucleation was then enhanced by 8 min of dc bias treatment in a 2% CH_4/H_2 gas mixture at a pressure of 20 mbar and a temperature of 780 °C.[21] Oriented diamond growth was performed during ten additional minutes at a pressure of 40 mbar.

A. Surface roughness: AFM investigations

As-received silicon substrates are covered by an up to 40 Å thick native oxide layer even after the cleaning procedure in acetone. As an amorphous SiO_x is not an adequate substrate for the growth of oriented diamond films, we removed the layer by heating the substrate up to 780 °C in a pure hydrogen plasma during 3 min at 20 mbar in the CVD reactor. With an etching rate of 20 Å per minute, 2 min etching is sufficient to clean the silicon. Three minutes are necessary to reach and stabilize the temperature of 780 °C. The hydrogen plasma etches the silicon substrate[22] and increases the surface roughness. Figure 1(a) shows the untreated substrate surface. The roughness of the surface is less than 1 nm (0.3 nm rms). After 3 min in a hydrogen plasma, the surface roughness increased by a factor of 4 (1.2-nm rms) and features with a diameter of 20–30 nm appeared [Fig. 1(b)]. They are due to the chemical etching of the silicon substrate by the hydrogen plasma.

After 15 additional minutes etching in a hydrogen plasma, the surface roughness increases to 10 nm rms. Hillocks with a diameter of 100 nm appear at the surface [Fig. 2(a)]. No CH_4 was introduced in the gas mixture in order to separate the effect of roughness and crystallite formation. However, if a dc bias voltage (-225 Vdc) is used during the etching, the roughness increases to 3 nm rms only and pits with a diameter of 100 nm appear on the surface with a density of 6×10^9 cm^{-2} [Fig. 2(b)]. This corresponds to the diamond nucleation density. However, no direct correlation between

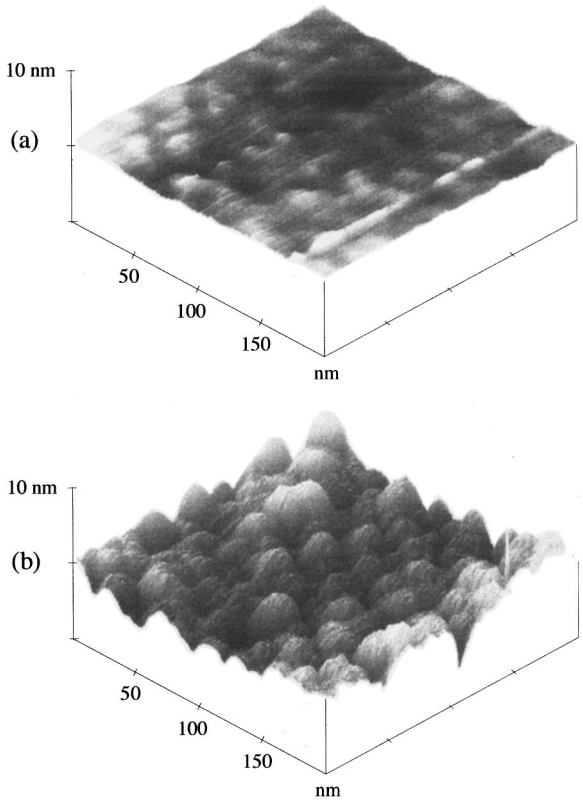

FIG. 1. AFM image of the (a) as received silicon surface, (b) silicon surface after 3 min in hydrogen plasma at 780 °C and 20 mbar.

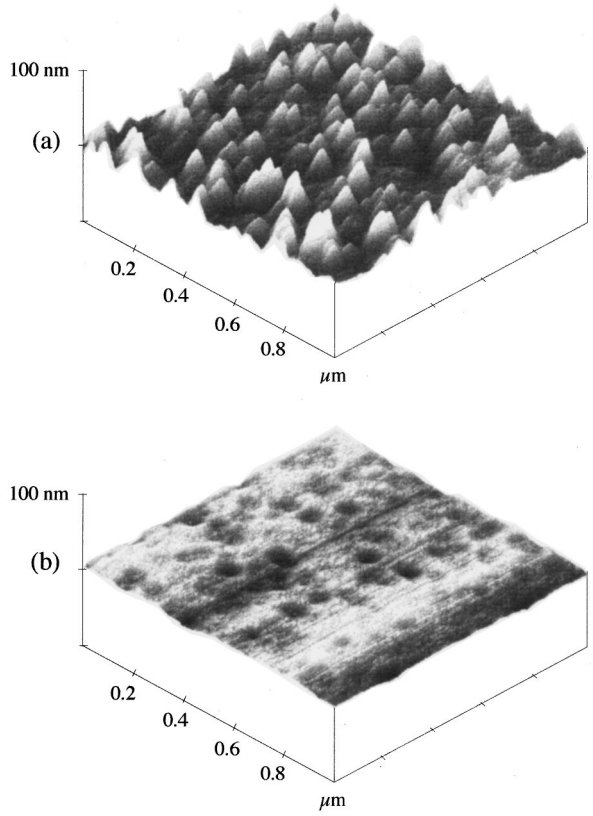

FIG. 2. AFM image of the (a) silicon surface after 15 min in hydrogen plasma at 780 °C and 20 mbar (no bias), (b) silicon surface after 15 min in hydrogen plasma at 780 °C and 20 mbar. The substrate was biased with −225 Vdc during the treatment. No CH_4 was introduced in the gas mixture in order to separate the effect of roughness and crystallite formation.

these pits and the nucleation sites can be drawn, unless we could prove the pits to be nucleation sites.[23]

B. Surface and interface orientation: Correlation between TEM and XPD investigations

As shown by AFM investigations, the silicon surface is rather rough before the enhanced nucleation step and the roughness increases during the biasing step (not shown). TEM measurements have been performed after the bias-enhanced nucleation step and the XPD measurements presented here have been done after ten additional minutes of oriented diamond growth (XPD diffractograms measured just after the bias-enhanced nucleation step show the same features[14]). Due to the polycrystalline nature of the film, the orientation of an overlayer with respect to the substrate can only be understood in terms of local heteroepitaxy or local orientation. The combination of TEM and XPD as it will be presented in the next paragraph is ideal for the investigation of the interface. While TEM is a very local probe, XPD averages the whole sample area and in addition, allows chemical information to be obtained.

1. TEM investigations

TEM bright-field investigations performed on the sample after the bias-enhanced nucleation step shows a high density of kinks defects in the silicon substrate (see Fig. 3). The defects are about 100 nm in diameter and two micrometers deep. The defects density is comparable to the density of pits shown by the AFM picture of Fig. 2(b). A correlation between the defects in the biased substrate and the pits due to the etching by the hydrogen plasma seems probable.

It is known from molecular-beam epitaxy techniques that the growth of β-SiC on silicon occurs by pit formation in the silicon substrate: with increasing deposition time, the silicon surface is covered by SiC which inhibits the silicon surface diffusion. The silicon atoms needed for the SiC growth are then provided by open areas on the surface leading to the

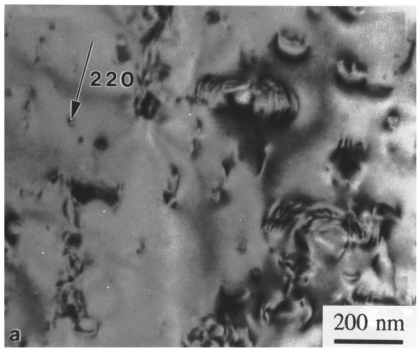

FIG. 3. (a) TEM bright-field image of the silicon substrate after 8 min of bias-enhanced nucleation. The [220] reflection of silicon is enhanced. The contrasts are due to strain fields from dislocation defects.

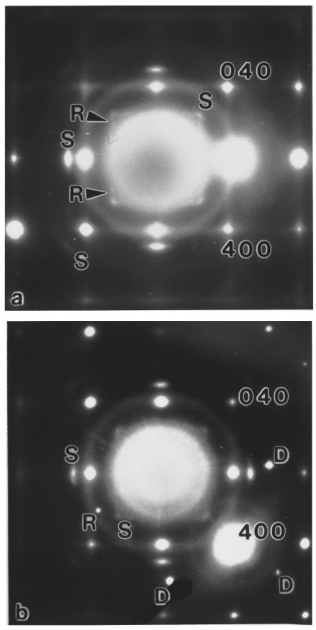

FIG. 4. (a) Electron-diffraction pattern of the substrate after 8 min of bias-enhanced nucleation. Silicon reflections are indexed. *S*: heteroepitaxial textured, nanocrystalline β-SiC; *R*: β-SiC [111] reflection. (b) Electron-diffraction pattern of a diamond crystallite. Silicon reflections are indexed. *S*: heteroepitaxial β-SiC; *D*: heteroepitaxial diamond; *R*: Diamond [111] reflection with no simple orientation relation with the substrate.

formation of pits.[24] Our AFM measurements indeed do not show an atomically flat β-SiC/Si interface.

But, our first TEM measurements did not show any correlation between the presence of defects in the silicon substrate and the presence of β-SiC. Moreover, as already mentioned, no evidence of diamond nucleation in these sites has been shown. Therefore, at present time, we cannot prove the direct correlation between the defects in the silicon substrate and the formation of β-SiC or the nucleation of diamond crystallites.

No continuous and homogeneous β-SiC layer was found on the substrate investigated by TEM. Partially oriented β-SiC nanocrystallites have been measured only. Figure 4(a) shows a TED pattern of a plan-view specimen from the silicon sample after the bias-enhanced nucleation step and Fig. 4(b) shows the TED pattern of a diamond crystallite. Silicon reflections are indexed. *S* stands for heteroepitaxial β-SiC nanocrystallites and *D* for heteroepitaxial oriented diamond. *R* points out the reflection without any simple orientation relation with the substrate. β-SiC and diamond show a preferential orientation with a weak tilt relative to the silicon substrate. The crystallites are partly composed by nonepitaxial oriented diamond phase (*R*). This is confirmed by the dark-field plane-view image where the bright crystals are surrounded by a darker halo (Fig. 5). Only the brightest part of the crystals is heteroepitaxial diamond. In conclusion, TED measurements performed after the bias-enhanced nucleation step point out the presence of mixed heteroepitaxial, nonepitaxial, and tilted diamond, respectively. β-SiC nanocrystallites on the silicon substrate.

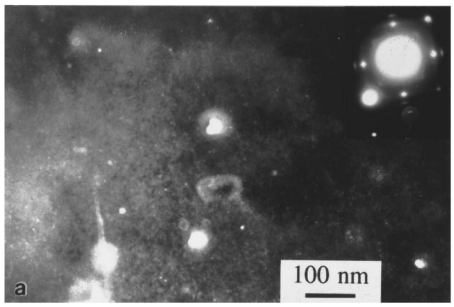

FIG. 5. Dark-field plan-view image of the silicon substrate after 8 min of bias-enhanced nucleation. The [220] reflection of diamond is enhanced. Only the brightest part of the crystallites is heteroepitaxial grown diamond.

2. XPD investigations

XPD is based on the forward focusing effect of electrons by atoms. So far, XPD was used by different groups to investigate single crystals and adsorbates on single crystals. When investigating the early growth stage of diamond on silicon, results have to be interpreted very carefully. The electrons are collected from many different, small crystallites, which have a small but finite dimension and interfere on the detector position. The measured diffracted signal is the sum of signals coming from all these crystallites.

By measuring and saving the C 1*s* peak and the Si 2*p* peak for all angles and with subsequent fitting, we get structural information about the growing diamond film, the SiC interface, and the underlying silicon substrate in one measurement. Figure 6 shows the fitted C 1*s* [Fig. 6(a)] and Si 2*p* [Fig. 6(b)] photoemission signals at normal incidence. The C 1*s* core-level peak shows a C-C component at 968.8 eV kinetic energy (KE) and a C-Si component at 970.1 eV. The Si 2*p* core-level peak shows a Si-Si component at 1154.6 eV KE and a Si-C component at 1153.3 eV. As the sample has been transferred to air, both peaks show a weak shoulder which reflects the oxygen contamination.

a. Orientation of the diamond crystallites with respect to the silicon (100) substrate. Figure 7 shows the four x-ray photoelectron diffractograms related to the fitted components of the XPS spectra. The four diffractograms have been normalized in order to enhance the intensity contrasts (intensity normalization over the azimuthal angles for each polar angle). The diffractogram of the C-C component of the C 1*s* peak is shown in Fig. 7(a). The major features of the diffractogram structure prove the preferential orientation of the growing diamond crystallites with respect to the (100) silicon substrate. As described in Ref. 14 this preferential orientation is already visible after few minutes of bias treatment. Figure 7(b) shows the diffractogram of the Si-Si component of the Si 2*p* peak. The structure of the diffractogram is similar to the one of clean (100) silicon[25] with the following restrictions: slightly smeared out features and a rapidly decreasing intensity with increasing polar angle (visible on the as-measured diffractogram before the normalization), both indicating the presence of a nonhomoepitaxial overlayer on top of the silicon substrate.[26] However, from the orientation of the different features in the diffractograms (Fig. 7) we can conclude that the diamond crystals are aligned with re-

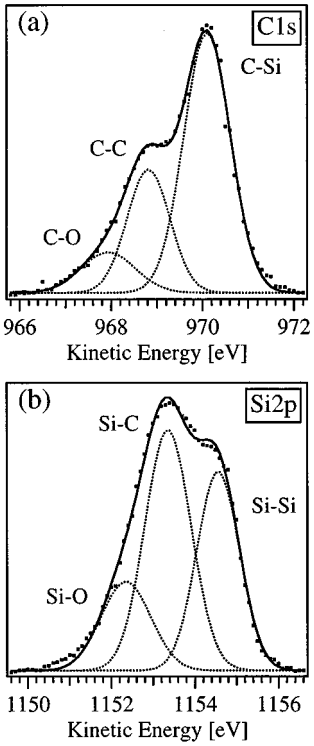

FIG. 6. (a) Fitted C 1*s* photoemission signal and (b) fitted Si 2*p* photoemission signal of the CVD diamond film after 8 min of bias-enhanced nucleation step and ten additional minutes of oriented growth.

spect to the silicon substrate. As we already proved the orientation of the β-SiC relative to the silicon (100) substrate,[14] the orientation of the diamond crystallites relative to the silicon is confirmed by HRSEM performed on the same substrate before the ten additional minutes of growth: Figure 8 shows parallel SiC stripe structures[10] and textured diamond crystallites. The stripe structure is not formed before the introduction of CH_4 in the gas mixture (not shown) and can thus be associated to β-SiC deposition. The β-SiC stripes are parallel to the silicon substrate lattice confirming the orientation of the β-SiC with respect to the substrate. The β-SiC stripes are seen all over the substrate surface proving the formation of a rather complete SiC layer during the early stage of growth.

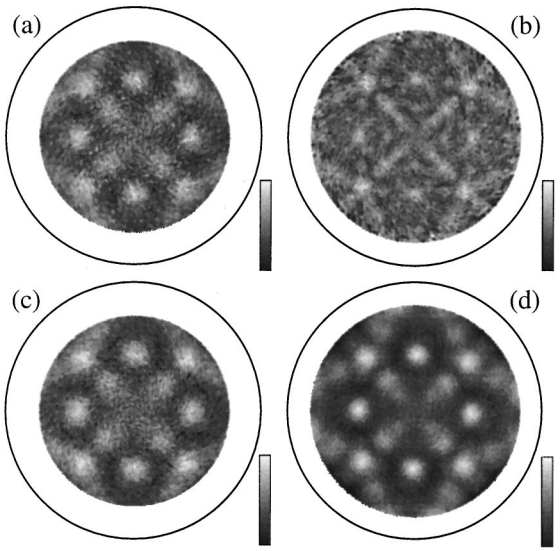

FIG. 7. Photoelectron diffractograms of the CVD diamond film after 8 min of bias-enhanced nucleation and 10 min of oriented growth. Diffraction pattern of the (a) fitted C-C component of the C 1*s* core-level signal, (b) fitted Si-Si component of the Si 2*p* core-level signal, (c) fitted C-Si component of the C 1*s* core-level signal, and (d) fitted Si-C component of the Si 2*p* core-level signal.

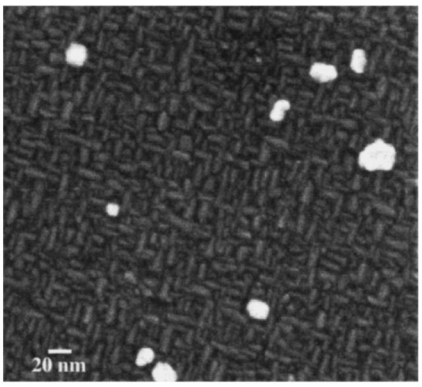

FIG. 8. HRSEM picture of the diamond crystallites after the bias-enhanced nucleation step.

The broad character of the maxima in the C-C diffractogram [Fig. 7(a)] are due to the weak scattering power of C atoms[20] (see below) and the weak preferential orientation of the diamond crystallites.[21] Hence, the existence of a tilt between the growing diamond lattice and the silicon substrate cannot be addressed.[27,28] However, our measurements absolutely rule out the experimental existence of the R45° theoretical model proposed by Verwoerd[29] consisting in the epitaxy of diamond on silicon (100) through a 45° rotation of the diamond lattice relative to the substrate. The C-C component diffractogram and the Si-Si component diffractogram are in phase involving no important azimuthal rotation of the diamond lattice relative to the silicon lattice.

b. Orientation of the β-SiC layer with respect to the silicon (100) substrate. We already discussed the formation of an oriented β-SiC layer or islands during the initial growth phase of diamond on silicon (100) in Ref. 14. The growth of heteroepitaxial β-SiC is confirmed by the diffractograms presented in Fig. 7(c) and Fig. 7(d). Figure 7(c) shows the diffraction pattern of the C-Si component fitted from the C 1*s* core-level peak while Fig. 7(d) shows the diffraction pattern of the Si-C component fitted from the Si 2*p* core-level peak. With an anisotropy of 30% $[I_{\max}-I_{\min}/I_{\max}]$ along the 54° polar angle, the β-SiC grown during the first minutes of oriented diamond deposition can be considered as well oriented [the anisotropy for the same polar angle on a β-SiC single crystal is 43% (Ref. 30)]. Both diffractograms show an orientation with respect to the (100) substrate allowing a structural investigation of the β-SiC through either the C 1*s* or the Si 2*p* peak. While the global features are similar for both diffractograms, we would like to focus on the fine-structure differences shown by these two diffractograms and on the comparison of the related SSC calculated diffraction patterns.

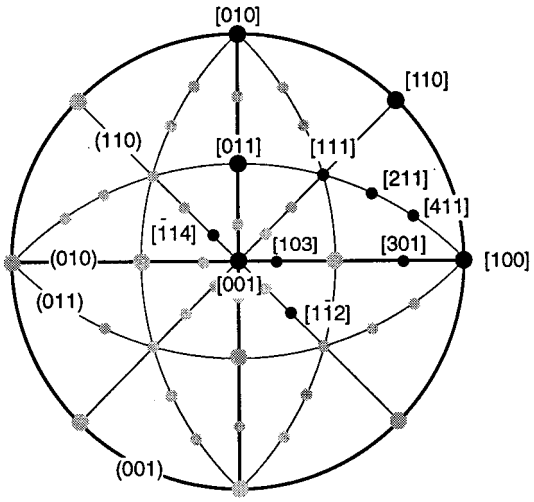

FIG. 9. Plot of the low index directions for the diffractograms of diamond, β-SiC, and silicon (100) surfaces.

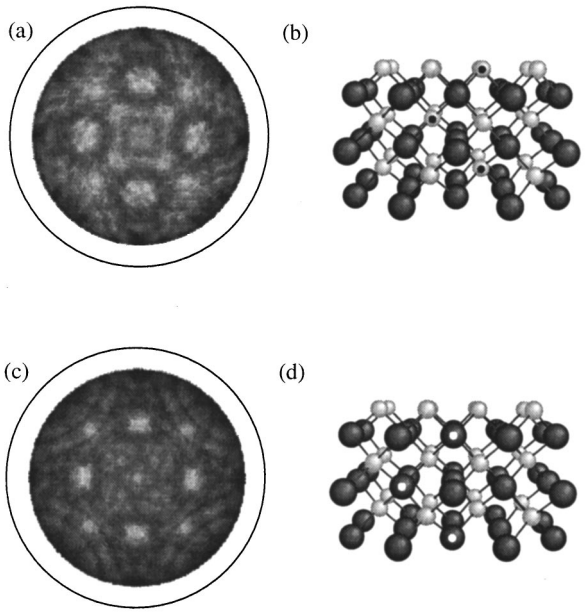

FIG. 10. β-SiC photoelectron diffractogram simulated by SSC theory calculations, (a) SSC diffractogram produced by carbon atoms photoemitters, (b) sketch of the carbon photoemitters position, (c) SSC diffractogram produced by silicon atoms photoemitters, (d) sketch of the silicon photoemitters position. The diffractograms have not been normalized.

While the C-Si diffraction pattern [Fig. 7(c)] shows rather smeared out features, the Si-C diffraction pattern shows much sharper details [Fig. 7(d)]. This is due to the kinetic energy of the collected electrons and the element dependence of the forward scattering and interference effect.[30] Silicon scatters about twice as much as carbon for forward-scattering directions which leads to important differences in the sharpness of the diffraction patterns. This is particularly evident if the maximum in the [110] direction at the polar angle of 45° is considered (low index directions are plotted in Fig. 9). In the [110] direction, an electron emitted by a carbon atom is only forward scattered by carbon atoms while an electron emitted by a silicon atom is forward scattered by silicon atoms. In Fig. 7(d), the relative sharpness of the [110] intensity maximum of the Si-C diffractogram is clear.

Our experimental results are in perfect agreement with the SSC calculations for SiC presented in Fig. 10. A cluster of 218 carbon and silicon atoms distributed over six layers has been used and the diffraction pattern has been produced by the emission from three carbon atoms in the case of Fig. 10(a) and three silicon atoms in the case of Fig. 10(c) distributed over three layers. The position of the carbon, respectively, silicon atoms is sketched in Fig. 10(b), respectively, 10(d). Two diffractograms rotated by 90° have been summed in order to simulate the presence of two β-SiC domains on the substrate[16] and the diffractograms have not been normalized. Comparing Figs. 10(a) and 10(c), it is clear that the diffractograms global features are similar but that the features of the Si-C simulated diffractogram [Fig. 10(c)] are sharper than the one of the C-Si simulated diffractogram [Fig. 10(a)].

c. The smeared out character of the C-C scattering pattern. The weak scattering power of the carbon atoms does not explain the lack of fine structure in the experimental diffractograms of the β-SiC and CVD diamond. In comparison with the SSC simulated β-SiC diffractogram and the (100) natural diamond diffractogram [see Fig. 14(a)], the diffractograms of Fig. 7 do not show any clear fine structure. The following considerations made for the C-C diffraction pattern can be extended to the β-SiC diffraction pattern without further restrictions. The smeared out features are due to the presence of nonoriented phases mixed to the oriented ones deposited on the silicon substrate, as measured by TED. Electrons of the slightly misaligned crystallites are averaged due to the large collecting area. Randomly oriented crystallites increase the overall background. These two effects are responsible for the rather fuzzy look of the diffractograms.

The presence of nonoriented crystallites is consistent with the HRSEM and the TED measurements (see Sec. III B) performed on the same substrate. A HRSEM picture is shown in Fig. 11. The nucleation density is 6.3×10^{8} cm^{-2} and only 30–40 % of the 60 nm large diamond crystallites are oriented with respect to the silicon substrate. This is consistent with literature data.[10,31] However, after 15 h of deposition, 80% of the diamond crystallites are oriented with respect to the substrate. As measured by XRD, the mean tilt of this thick diamond film is only 5° relative to the substrate. The

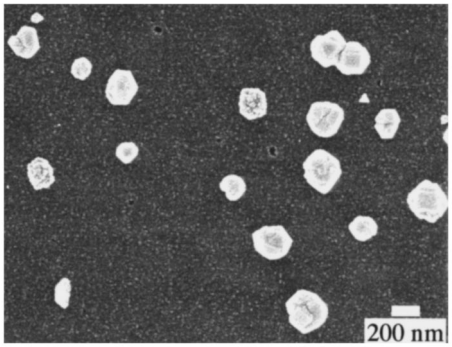

FIG. 11. HRSEM picture of the diamond crystallites after the bias-enhanced nucleation step and ten additional minutes of deposition under typical conditions for oriented growth.

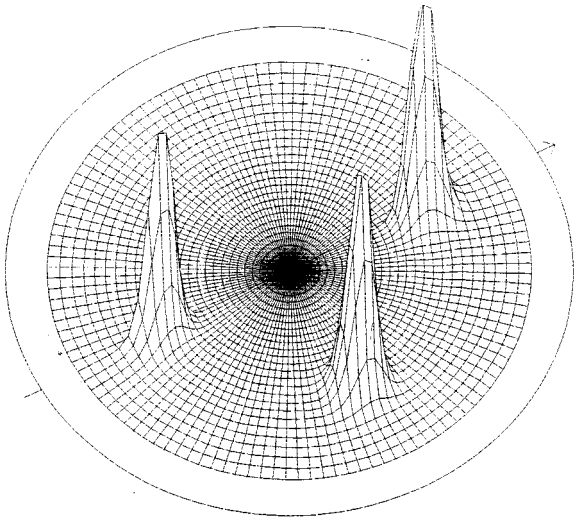

FIG. 12. [111] x-ray half-pole figure of the diamond film after 15 h of oriented growth.

pure rotational misorientation is only 4°.[32] The XRD half-pole figure measured for the [111] diamond reflection is shown in Fig. 12 and proves the very good orientation of the 10 μm thick diamond film.

Our results are in good agreement with the model of evolutionary selection of specific crystallite orientations by Van der Drift.[3,33] A low percentage of oriented crystallites at the beginning of the growth can be changed to a highly oriented film by choosing adequate deposition parameters. However, there is a limit to the minimum amount of oriented crystallites necessary at the beginning. In Fig. 13(a) we show the diffractogram of a sample which was only submitted to a nucleation enhancing treatment at 800 °C during 8 min. No

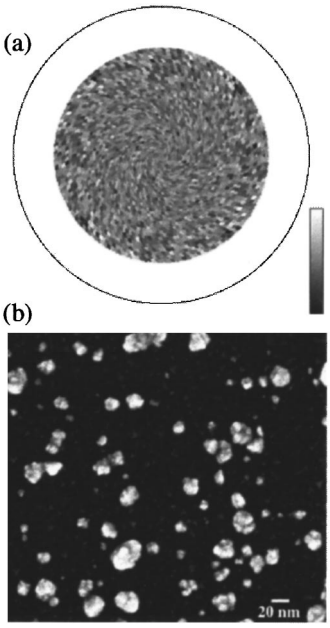

FIG. 13. (a) Photoelectron diffractograms of the CVD diamond film after 8 min of bias-enhanced nucleation without previous heating in hydrogen plasma, (b) HRSEM picture of the same substrate.

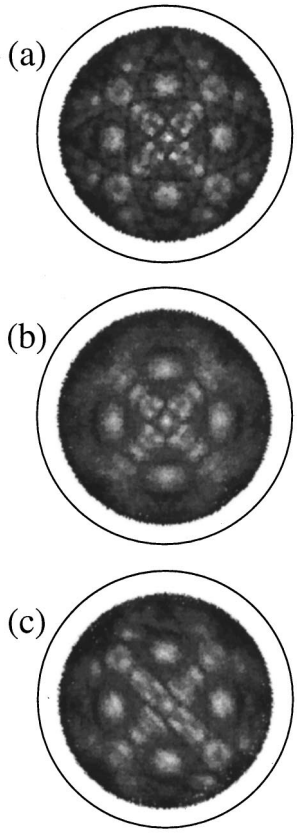

FIG. 14. (a) Stereographic projection of the C 1*s* XPD intensity at 968.8-eV KE of a natural (100) diamond surface. Simulations of the misorientation of the diamond crystallites by tilting and azimuthally rotating the diffractogram in (a). (b) Simulations of the azimuthal rotation, $\Delta\phi = \pm 8°$ and (c) simulations of the tilting of the diamond crystallites, $\Delta\theta = \pm 6°$.

structure can be seen and in the HRSEM picture [Fig. 13(b)] no orientation of the crystallites can be recognized.

Simulations of the misorientation of the diamond crystallites have been performed by tilting ($\Delta\theta$) and azimuthaly rotating ($\Delta\phi$) the experimental (100) natural diamond diffractogram shown in Fig. 14(a).[20] The resulting diffractograms were summed and arithmetically averaged using 30% of well-oriented CVD diamond diffractograms and 70% of tilted or rotated diffractograms. The result is presented in Fig. 14(b). The fine structure is still visible even for an azimuthal rotation of $\Delta\phi = \pm 8°$. The intensity maxima are much broader than the experimental ones [Fig. 7(a)]. Simulations of the tilting of the diamond crystallites [Fig. 14(c)] are a better approximation of the experimental diffractogram except that the [112] and [103] maxima (low index directions plotted in Fig. 9) are distinct even for $\Delta\phi = \pm 6°$. A combination of both effects does not produce a better agreement with the experimental diffractogram. It seems that other effects may play a significant role.

The best simulations have been obtained by rotating the SSC calculated diffractogram for a 5 ML diamond cluster[16] shown in Fig. 15(a) with a tilt of $\Delta\phi = \pm 6°$. The resulting diffractogram is shown in Fig. 15(b). The global features and the intensity maxima are similar except for the [103] direction where the experimental intensity is weaker than the calculated one and for the curved bandlike structures centered

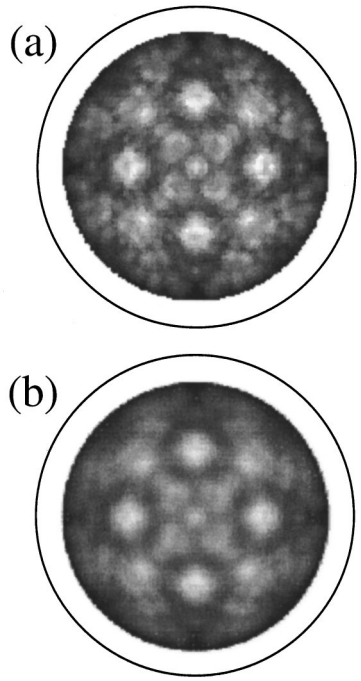

FIG. 15. (a) Photoelectron diffractogram of a 5 ML carbon atoms cluster simulated by SSC theory calculations. (b) Tilted SSC simulated photoelectron diffractogram, $\Delta\theta = \pm 6°$. The diffractograms have not been normalized.

along the projection of dense crystal planes which are absent from the experimental diffractogram. The lack of such features is typical for a long-range disorder. The good agreement of the experimental diffractogram with the rotated SSC 5-ML cluster diffractogram does not mean that the diamond crystallites are only 5 ML thick, but that no longer range order exists in the diamond lattice at this early growth stage due to the high density of misfit dislocations. This short range order is not sufficient to produce a low-energy electron diffraction (LEED) pattern.

The situation is different for an oriented diamond film grown during 15 h: the diffraction features typical for a long-range order (high index intensity maxima and weak curved bandlike structures) are visible despite of the smearing out of the pattern [Fig. 16(a)]. LEED shows broad spots [Fig. 16(b)]. The pattern does not allow a distinction between a (2×1) and an (1×1) reconstruction.

C. Surface composition: correlated XPS and HRSEM investigations

The HRSEM measurements of the substrate after 8 min of dc bias treatment and ten additional minutes of oriented diamond growth allows us to get quantitative information on the carbon phases present at the surface. HRSEM quantification have been compared to XPS studies of the surface. The amount of carbon calculated with HRSEM (Fig. 11) on the basis of a nucleation density of 6.3×10^{8} cm^{-2} and an average nuclei surface of 3.6×10^{3} nm^{2} is 7–10 times smaller than the amount of carbon phases calculated on the basis of XPS measurements (Fig. 6). We conclude that the major part of carbon present on the sample is not in the form of diamond nuclei. We suppose the existence of carbon domains

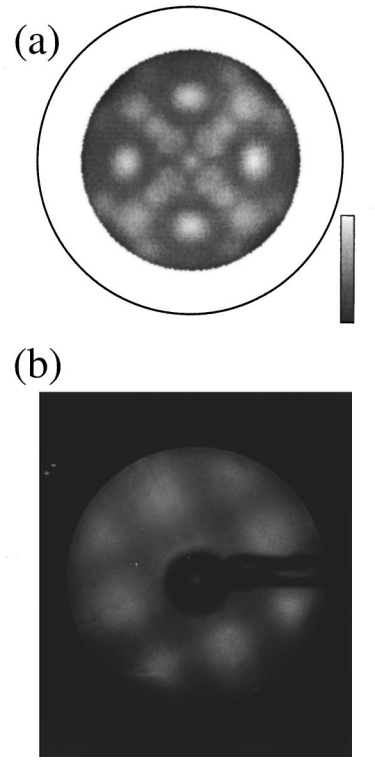

FIG. 16. (a) Stereographic projection of the C 1*s* XPD intensity at 968-eV KE of a CVD (100) diamond surface after 15 h of growth. (b) LEED pattern of the same surface (102.9-eV electron energy).

which are too small to be detected by HRSEM but are detected by XPS. It seems that these C-C domains are too small to be or become diamond nuclei and are then etched away by the hydrogen plasma during the growth process. Further confirmation stems from the fact that the nondiamond phase decreases rapidly with deposition time. This is suggesting the existence of a critical radius of the nuclei.[11] If the nuclei has not reached this size before the end of the bias treatment, it will be etched away during the growth process. However, we are not able to estimate the size of these domains and to tell without doubt if they have the diamond structure or not. Using a combination of AFM and STM, we are able to investigate the topography and the conductivity of the surface in one measurement. Preliminary analysis confirm the presence of small domains on the surface of the silicon substrate, which conductivity is different from the substrate and the diamond crystallites conductivity. Figure 17(a) shows the topography of the sample after the bias treatment with one crystallite of 170 nm in diameter. Figure 17(b) shows the current map of the same place on the substrate. All around the crystallite, which presents a bad conductivity (black, minimal current through the tip is 60 pA), small domains with differences in conductivity (gray to white, maximal current through the tip is 600 pA) are disposed. As the measured current depends on the tip gold coverage, we cannot specify the chemical species present on the surface. Therefore, this measurement does not consist in an indisputable proof of the existence of nondiamond carbon domains on the surface but confirms the presence on the surface of domains which conductivities are different from the diamond conductivity.

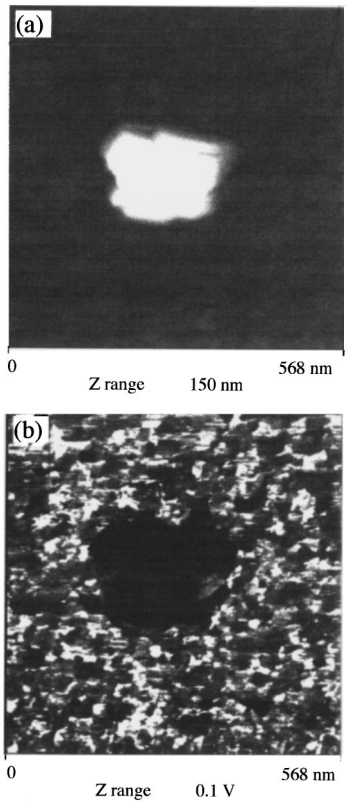

FIG. 17. AFM/STM combination. (a) Topography of the sample after the bias treatment: one crystallite of 170 nm in diameter. (b) Current map of the same place on the sample. Black color stands for a bad conductivity ($I=60$ pA) and white color for a good conductivity ($I=600$ pA): small domains with differences in conductivity are visible all around the diamond crystallite.

IV. CONCLUSIONS

Surface roughness study of the silicon substrate at the beginning of the plasma process and after the bias-enhanced nucleation step has been investigated. The hydrogen plasma treatment increases the surface roughness by a factor of ten. Associated to a bias application, the hydrogen plasma produces pits on the substrate surface. No correlation between these pits and nucleation sites can be drawn.

The preferential orientation of β-SiC grown on silicon (100) during the first minutes of deposition has been proved by HRSEM and XPD. HRSEM shows that the β-SiC forms a rather complete layer on the silicon (100) and XPD shows that the orientation of the layer is not perfect.

The preferential orientation of the diamond crystallites with respect to the silicon substrate at an early growth stage has been studied by TEM, HRSEM, and XPD, and quantified by comparison of HRSEM pictures and experimental scattering patterns. At this early stage of growth, only 30–40% of the crystallites have been found to be oriented relative to the substrate. However, after 15 h of deposition, 80% of the diamond crystallites are oriented with respect to the substrate. The tilt measured by XRD is then of 5°. This is consistent with the model of evolutionary selection of specific crystallite orientations by Van der Drift.

Simulations of diffraction patterns induced by tilted and azimuthally rotated diamond crystallites have been performed in order to reproduce the lack of fine structure in the experimental diffractogram. Conclusions leading to the existence of a short-range order (not more than 5 ML) in the lattice of the diamond nanocrystallites after few minutes of growth have been drawn.

The structure of the β-SiC interface has been investigated through the fitted C-Si component of the C 1*s* peak diffractogram and through the fitted Si-C component of the Si 2*p* peak diffractogram. Differences in the diffraction features have been studied and found to be due to the kinetic energy and the element dependence of the forward scattering. The amount of carbon on the silicon substrate has been measured by XPS and HRSEM. Comparing the results, we postulated the existence of carbon islands which are too small to be or become diamond nuclei and are then etched away by the hydrogen plasma during the growth process. The size and the nature of these islands are not clear. A preliminary study by STM/AFM has been done and confirms the existence of domains, the conductivity of which is different from the diamond and the silicon ones.

ACKNOWLEDGMENTS

We wish to thank Dr. P. Walther from Laboratory of Electron Microscopy (ETHZ) for performing the high-resolution SEM measurements and Dr. C. Hellwig from EMPA for performing the XRD analysis. This work forms part of a joint project with CSEM in Neuchâtel and EMPA in Dübendorf. The authors gratefully acknowledge financial support by the Swiss National Science Foundation. It was carried out under the auspices of the trinational ''D-A-CH'' cooperation of Germany, Austria and Switzerland on the ''Synthesis of Superhard Materials.''

*Present address: Department of Physics, North Carolina State University, Raleigh NC 27695. Electronic address: maillard@unity.ncsu.edu

[1] H. Liu and D. S. Dandy, Diamond Relat. Mater. **4**, 1173 (1995).
[2] S. D. Wolter, B. R. Stoner, J. T. Glass, P. J. Ellis, D. S. Buhaenko, C. E. Jenkis, and P. Southworth, Appl. Phys. Lett. **62**, 1215 (1993).
[3] C. Wild, P. Koidl, W. Müller-Sebert, H. Walcher, R. Kohl, N. Herres, R. Locher, and R. Brenn, Diamond Relat. Mater. **2**, 158 (1993).
[4] X. Jiang, C. P. Klages, R. Zachai, M. Hartweg, and H. J. Fuesser, Appl. Phys. Lett. **62**, 3438 (1993).
[5] B. R. Stoner, S. R. Sahaida, J. P. Bade, P. Southworth, and J. Ellis, J. Mater. Res. **8**, 1334 (1993).
[6] T. Taschiniba, K. Hayashi, and K. Kobashi, Appl. Phys. Lett. **68**, 1491 (1996).
[7] S. D. Wolter, T. H. Borst, A. Vescan, and E. Kohn, Appl. Phys. Lett. **68**, 3558 (1996).
[8] R. Kohl, C. Wild, N. Herres, P. Koidl, B. R. Stoner, and J. T. Glass, Appl. Phys. Lett. **63**, 1792 (1993).
[9] X. Jiang and C. L. Jia, Appl. Phys. Lett. **67**, 1197 (1995).
[10] T. Suesada, N. Nakamura, H. Nagasawa, and H. Kawarada, Jpn. J. Appl. Phys. **34**, 4898 (1995).

[11] X. Jiang, K. Schiffmann, A. Westphal, and C. P. Klages, Appl. Phys. Lett. **63**, 1203 (1993).
[12] C. L. Jia, K. Urban, and X. Jiang, Phys. Rev. B **52**, 5164 (1995).
[13] M. A. George, A. Burger, W. E. Collins, J. L. Davidson, A. V. Barnes, and N. H. Tolk, J. Appl. Phys. **76**, 4099 (1994).
[14] E. Maillard-Schaller, O. M. Küttel, P. Gröning, P. Aebi, and L. Schlapbach (unpublished).
[15] J. Osterwalder, T. Greber, A. Stuck, and L. Schlapbach, Phys. Rev. B **44**, 13 764 (1991).
[16] E. Maillard-Schaller, O. M. Küttel, and L. Schlapbach, Phys. Status Solidi A **153**, 415 (1996).
[17] C. S. Fadley, in *Syncrotron Radiation Research: Advances in Surface Science*, edited by R. Z. Bachrach (Plenum, New York, 1992), Chap. 11.
[18] P. A. Lee, Phys. Rev. B **13**, 5261 (1976).
[19] S. Kono, S. M. Goldberg, N. F. T. Hall, and C. S. Fadley, Phys. Rev. B **22**, 6085 (1980).
[20] O. M. Küttel, R. G. Agostino, R. Fasel, J. Osterwalder, and L. Schlapbach, Surf. Sci. **312**, 131 (1994).
[21] E. Schaller, O. M. Küttel, P. Aebi, and L. Schlapbach, Appl. Phys. Lett. **67**, 1533 (1995).
[22] G. M. Fuchs, G. Friedbacher, D. Schwarzbach, E. Bouveresse, M. Grasserbauer, R. Haubner, and B. Lux, J. Anal. Chem. **353**, 698 (1995).
[23] R. W. Cahn, Nature (London) **375**, 363 (1995).
[24] K. Zekentes, V. Papaioannou, B. Pecz, and J. Stoemenos, J. Cryst. Growth **157**, 392 (1995).
[25] E. Schaller, O. M. Küttel, R. G. Agostino, and L. Schlapbach, *Proceedings of the 3rd Applied Diamond Conference, Gaithersburg USA, August 1995*, NIST Special Publication (NIST, Washington, 1995), Vol. 885, p. 325.
[26] R. G. Agostino, O. M. Küttel, P. Aebi, R. Fasel, J. Osterwalder, and L. Schlapbach, J. Appl. Phys. **80**, 2131 (1996).
[27] S. Geier, R. Hessmer, U. Preckwinkel, D. Schweitzer, M. Schreck, and B. Rauschenbach, J. Appl. Phys. **79**, 1907 (1996).
[28] K. Schiffmann and X. Jiang, Appl. Phys. A **59**, 17 (1994).
[29] W. S. Verwoerd, Surf. Sci. **404**, 24 (1994).
[30] S. Juillaguet, L. Kubler, M. Diani, J. L. Bischoff, G. Gewinner, P. Wetzel, and N. Bécourt, Surf. Sci. **339**, 363 (1995).
[31] X. Jiang and C. P. Klages, *New Diamond and Diamond-Like Films*, edited by P. Vincenzini (Elsevier, Lausanne, 1995), p. 23.
[32] R. Hessmer, M. Schreck, S. Geier, B. Rauschenbach, and B. Stritzker, Diamond Relat. Mater. **4**, 410 (1995).
[33] A. Van der Drift, Philips Res. Rep. **22**, 267 (1967).